# Current-enabled optical conductivity of superconductors

Michał Papaj and Joel E. Moore

Phys. Rev. B **106**, L220504 — Published 20 December 2022

DOI: 10.1103/PhysRevB.106.L220504

# Current-enabled optical conductivity of superconductors

Michał Papaj
*Department of Physics, University of California, Berkeley, CA 94720, USA*

Joel E. Moore
*Department of Physics, University of California, Berkeley, CA 94720, USA and*
*Materials Sciences Division, Lawrence Berkeley National Laboratory, Berkeley, CA 94720, USA*

In most superconductors, optical excitations require impurity scattering or the presence of multiple bands. This is because in clean single-band superconductors, the combination of particle-hole and inversion symmetries prevents momentum-conserving transitions. In this work we show how the flow of supercurrent can lead to new contributions to optical conductivity. As supercurrent breaks inversion symmetry, transitions across the superconducting gap become allowed even in clean superconductors and dominate over impurity-induced contributions for energies comparable to the gap width. The response is dependent on the nature of the underlying normal state as well as on the type of superconducting order. Use of an external magnetic field to produce a screening supercurrent, with controllable magnitude and direction, enables a detailed investigation of the superconducting state, allowing determination of the gap symmetry in unconventional superconductors for which other techniques have not been practicable.

*Introduction.*— Optical measurements are well established as one of the most fundamental experimental techniques for studies of quantum materials [1, 2]. Properties such as reflectivity and transmissivity can shed light on the electronic structure of solids and enable characterization of ordered phases in many systems [3]. In particular, optical measurements can give insight into the nature of the superconducting state, for example by determination of the superconducting gap size [4–6]. On the theoretical level, optical properties can be characterized by the optical conductivity $\sigma(\omega)$, which can be obtained from microscopic considerations. In the case of superconductors, such a description has been provided by Mattis and Bardeen [7], who have analyzed the problem in the dirty limit, where the superconducting coherence length $\xi_0$ is much larger than the mean free path $l$. In this limit the optical response largely follows the normal state Drude conductivity for $\hbar\omega \gg 2\Delta$, where $\Delta$ is the magnitude of the superconducting order parameter. However, the real part of $\sigma(\omega)$ becomes suppressed for smaller frequencies and vanishes for $\hbar\omega \leq 2\Delta$. This theory, together with its extensions to arbitrary purity [8, 9], has been very successful in explaining the optical properties of many superconductors.

The reasons for the considerable success of Mattis-Bardeen results even beyond the dirty limit have recently been elucidated in a theory for optical transitions of clean, multiband superconductors [10]. Those authors have shown that, due to a combination of inversion and particle-hole symmetries, a selection rule forbids momentum-conserving optical transitions across the superconducting gap in simple single-band superconductors. They have also shown that when multiple bands are present, some transitions become allowed, giving rise to new optical conductivity contributions that can dominate over Mattis-Bardeen terms in very clean systems ($l \gg \xi_0$), such as FeSe. Moreover, it can be shown that when a superconductor breaks inversion symmetry, optical transitions become allowed and the material will exhibit a variety of linear and nonlinear optical effects [11]. While intrinsic inversion-breaking superconductors are rare, another opportunity for breaking inversion opens up when we consider supercurrent flow through the material, as currents are known to strongly affect the optical properties of other materials, such as Dirac and Weyl semimetals [12].

In this work, we investigate the effect of an inversion-breaking supercurrent on the optical conductivity of superconductors. We demonstrate that optical transitions are possible even in clean, single-band superconductors when a supercurrent flow is introduced. By treating optical conductivity at the linear response level, we show that the predicted signal depends on the nature of the normal state as well as the type of superconducting order. This is corroborated by the comparison of supercurrent-induced responses between single band and Dirac fermion systems, and between s-wave and d-wave pairings. The predicted optical response dominates over that of Mattis-Bardeen theory for photon energies in the vicinity of the superconducting gap edge. As the supercurrent flow can be established and controlled by applying external magnetic field through the Meissner effect, this approach introduces a control knob that can modify an optical response of a superconductor in an experimental setting without requiring the system to be driven far from equilibrium. Combining these factors leads to a promising tool for investigation of the superconducting state.

*Supercurrent and the excitation spectrum.*— When a supercurrent flow is introduced in a superconductor, the Cooper pairs in the condensate acquire finite momentum $2\mathbf{q}$. As a result, the dispersion of quasiparticle excitations

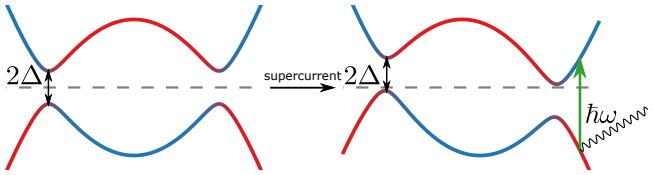


FIG. 1. The effect of supercurrent on quasiparticle dispersion. In the absence of supercurrent, transitions across the superconducting gap are forbidden. However, inversion breaking due to the current flow enables transitions that contribute to interband optical conductivity. Blue and red colors indicate degree of superposition between particle and hole-like states.

now includes a term corresponding to a Doppler shift [13]:

$$E(\mathbf{k}) = \sqrt{\xi_{\mathbf{k}}^2 + \Delta^2} + v_{\mathbf{k}} \cdot \mathbf{q}, \tag{1}$$

with $\xi_{\mathbf{k}} = \epsilon_{\mathbf{k}} - \mu$, where $\epsilon_{\mathbf{k}}$ is the particle dispersion in the normal state, $\mu$ is the chemical potential, $\Delta$ is the superconducting order parameter, and $v_{\mathbf{k}} = \partial\epsilon_{\mathbf{k}}/\partial\mathbf{k}$ is the group velocity. As the Cooper pair momentum $2\mathbf{q}$ is determined by the direction of the supercurrent, the quasiparticle energy increases or decreases, depending whether it moves parallel or anti-parallel to the current. Therefore, supercurrent flow introduces anisotropy into the quasiparticle dispersion, leading in simple cases to tilting of the spectrum. This is presented in Fig. 1, which shows the Bogoliubov-de Gennes (BdG) spectrum around the superconducting gap. When the Cooper pair momentum exceeds a critical value, Eq. (1) allows for zero-energy excitations. This leads to the appearance of a segmented Fermi surface, which has recently been observed in thin films of 3D topological insulators under proximity effect [14] and can lead to topological phase transition [15, 16]. A related phenomenon in which the Doppler effect plays a role is the Volovik effect [17], where the supercurrent in vortices leads to changes in the density of states. This effect has been discussed and detected in optical measurements previously [18–20]. However, in our case we are concerned with small in-plane magnetic fields that do not lead to formation of vortices. Supercurrent-induced effects were also explored in the context of infrared activation of the Higgs mode in superconductors [21, 22].

The supercurrent flow can arise either due to an explicit transport current or due to an external applied magnetic field [23]. In the latter case, as a result of the Meissner effect, a screening supercurrent develops at the surface of the superconductor. This screening supercurrent is directly connected to the magnetic vector potential $\mathbf{A}$ via the London equation:

$$\mathbf{j}_S = -\frac{n_S e^2}{m}\mathbf{A}, \tag{2}$$

where $n_S$ is the superfluid density, $e$ is the electron charge and $m$ is the electron mass. The behavior of $\mathbf{A}$ at the surface of a superconductor can be determined by combining London and Maxwell equations. Assuming that the boundary of the superconductor is at the $z = 0$ plane and the supercurrent flows along $\hat{\mathbf{x}}$, in the London gauge ($\nabla \cdot \mathbf{A} = 0$) the vector potential will only have a non-zero $x$ component. At the surface the vector potential can thus be determined to be $A_x(z = 0) = B_{\text{ext}}\lambda_L$, where $B_{ext}$ is the magnitude of the external magnetic field, which is pointing along $\hat{\mathbf{y}}$ ($\mathbf{B}(z > 0) = B_{\text{ext}}\hat{\mathbf{y}}$), and $\lambda_L$ is the London penetration depth. Therefore, in order to obtain a larger Cooper pair momentum $2q = 2eB_{\text{ext}}\lambda_L$ due to the external magnetic field, one should increase the external magnetic field and use superconductors with longer $\lambda_L$. With Cooper pair momentum and supercurrent present, the inversion symmetry is broken and we can now investigate the new contributions to optical conductivity.

*Superconductor models.*— In this work we focus on two different models of superconductors that exemplify the different aspects of supercurrent-enabled optical conductivity. To study these types of superconductors, we employ the BdG formalism to calculate the Matsubara Green's functions as discussed below. We obtain results for a single-band spin degenerate s-wave superconductor and for a Dirac fermion under proximity effect from an s-wave superconductor. The results can also be extended to d-wave superconductors as shown in Supplemental Materials [24] (see, also, references [25, 26] therein). The mean-field Hamiltonian is assumed to arise from an interacting Hamiltonian $H = \sum_{\mathbf{k}\sigma} \xi_{\mathbf{k}} c^\dagger_{\mathbf{k}\sigma} c_{\mathbf{k}\sigma} + \sum \lambda_{\mathbf{q}} c^\dagger_{\mathbf{k}+\mathbf{q}\sigma} c^\dagger_{\mathbf{k}'-\mathbf{q}\sigma'} c_{\mathbf{k}'\sigma'} c_{\mathbf{k}\sigma}$, leading to a gap equation at zero temperature:

$$\Delta_{\mathbf{k}} = -\sum_{\mathbf{p}} \lambda_{\mathbf{k}-\mathbf{p}} \frac{\Delta_{\mathbf{p}}}{2\sqrt{\xi_{\mathbf{p}}^2 + \Delta_{\mathbf{p}}^2}} \tag{3}$$

In the s-wave case, the interaction strength is momentum-independent, $\lambda_{\mathbf{p}} = \lambda$, and in consequence the superconducting order parameter is also momentum-independent, $\Delta_{\mathbf{k}} = \Delta$.

In each case, the influence of the supercurrent is introduced by including the vector potential using minimal coupling $k_i \to k_i + q_i\tau_z$, where $\tau_z = \pm 1$ for particle and hole sectors of the mean-field BdG Hamiltonian. In all of the following calculations we will assume that the supercurrent, and thus the Cooper pair momentum, is directed along the $x$ axis and so $\mathbf{q} = q_x\hat{x}$. In the case of our analytical solution for the optical conductivity of proximitized Dirac fermions, we do not solve for the superconducting order parameter self-consistently when supercurrent is present. Still, for small supercurrents this should not introduce qualitative differences [27], which we also verify numerically in the tight-binding model.

The most generic model of a superconductor that we consider consists of a single spin-degenerate tight-binding band with nearest-neighbor hopping $t$ on a square lattice

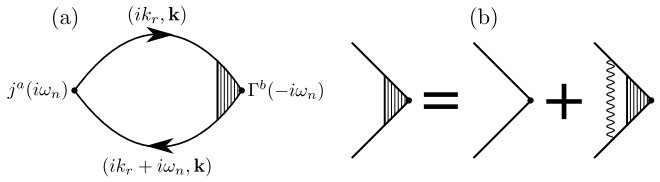


FIG. 2. Feynman diagrams in Matsubara formalism. (a) Current-current correlation function evaluated using a bubble diagram with vertex correction to ensure satisfaction of Ward identities. (b) Self-consistent equation for the vertex correction. The straight lines indicate propagators in Matsubara formalism, and the wiggly line indicates the interaction that leads to superconducting pairing.

with unit lattice constant at chemical potential $\mu$ with a superconducting gap $\Delta$:

$$H^{\mathrm{TB}}_{\mathrm{BdG}}(\mathbf{k}) = (t(2 - \cos(k_x) - \cos(k_y)) - \mu)\,\tau_z + \Delta\tau_x \quad (4)$$

Such a simple model can nevertheless fully demonstrate the supercurrent-induced optical conductivity.

For the purpose of an analytical derivation, we also consider a Dirac fermion with s-wave superconducting order parameter:

$$H^{\mathrm{D}}_{\mathrm{BdG}}(\mathbf{k}) = (\hbar v k_x s_y - \hbar v k_y s_x - \mu)\,\tau_z + \Delta\tau_x \quad (5)$$

where $s_i$ are Pauli matrices representing the spin degree of freedom. This model can describe the surface state of a 3D topological insulator under the proximity effect from a conventional superconductor, as in the case of the recent experiment reporting observation of a segmented Fermi surface [14]. In such a scenario, the Fermi energy is placed high above the Dirac point, and so for small photon energies we can focus only on the upper Dirac cone around the superconducting gap. This allows us to treat this system as effectively a single-band superconductor with a helical spin-texture [24].

*Formalism.*— To obtain the optical conductivity $\sigma_{ab}(\omega)$ we work within linear response using the Kubo formula in Matsubara formalism adapted to the BdG approach. This corresponds to evaluation of the current-current correlation function as depicted in Fig. 2(a). Expressed in terms of Matsubara Green's functions this gives [28]:

$$\Pi_{ab}(i\omega_n) = -\frac{1}{\beta V}\sum_{\mathbf{k},ik_r} \mathrm{Tr}\, j^a_0 G_0(\mathbf{k}, ik_r + i\omega_n)\Gamma^b(i\omega_n)G_0(\mathbf{k}, ik_r), \quad (6)$$

where $j^a_0$ is the component of the bare current operator for the BdG Hamiltonian as described below, $\Gamma_b$ is the current operator with the vertex correction included, and $G_0(\mathbf{k}, ik_n) = (ik_n - H_{\mathrm{BdG}})^{-1}$ is the Matsubara Green's function for the BdG Hamiltonian. We are focusing here on the transitions across the superconducting gap in the AC regime, but $\sigma(\omega)$ will also have a DC component given by $\delta(\omega)$. Using Eq. (6) we can obtain the real (dissipative) part of the optical conductivity by analytic continuation:

$$\mathrm{Re}\,\sigma_{ab}(\omega) = \frac{1}{\omega}\mathrm{Im}\Pi_{ab}(\omega + i\eta) \quad (7)$$

The vertex correction $\Gamma$ is crucial in the consideration of optical responses in the presence of the supercurrent, as it ensures the satisfaction of Ward identities and in turn that the obtained results are physical. Indeed, calculating the uncorrected current-current correlation function for the case of supercurrent flow in a system with a parabolic band yields a non-zero result [24]. However, since the system with a parabolic band is Galilean invariant, the current operator is proportional to momentum $\mathbf{j}_0 \sim \mathbf{k}$, which means it commutes with the full interacting Hamiltonian $[j^a_0, H] = 0$. Therefore, no non-trivial optical response is possible. In order to rectify this issue, we include the vertex correction at the ladder approximation level, which constitutes an appropriate conserving approximation for the superconductivity treated at the mean-field level [29, 30]. Such a vertex correction is depicted in Fig. 2(b) and corresponds to the following self-consistent equation:

$$\Gamma^a(i\omega_n) = j^a_0 - \frac{\lambda}{\beta V}\sum_{\mathbf{k},ik_r} \tau_z G_0(\mathbf{k}, ik_r + i\omega_n)\Gamma^a(i\omega_n)G_0(\mathbf{k}, ik_r)\tau_z \quad (8)$$

For the s-wave case, since the interaction strength is momentum-independent, the correction to the vertex is only a function of frequency, constant in momentum space.

The bare current operators in each of the models are calculated including an infinitesimal vector potential perturbation $\delta\mathbf{A}$ in the normal state Hamiltonians in particle-hole space according to minimal coupling rule $\mathbf{k} \to \mathbf{k} - e\delta\mathbf{A}\tau_z$, where $\tau_z = \pm 1$ for particle and hole sectors of the BdG Hamiltonian. By taking an appropriate derivative we arrive at the current operator in a given direction:

$$j^a_0 = -\left.\frac{\partial H_{\mathrm{BdG}}(\mathbf{k} - e\delta\mathbf{A}\tau_z)}{\partial \delta A_a}\right|_{\delta\mathbf{A}=0,\Delta=0} \quad (9)$$

*Optical conductivity results.*— We can now employ the formalism described above to obtain the real part of the optical conductivity. Since the s-wave superconductors have no Fermi surface for small Cooper pair momenta, only the interband contribution is relevant to their optical conductivity at $T = 0$. We begin with the proximitized Dirac fermion as the analytical result allows for

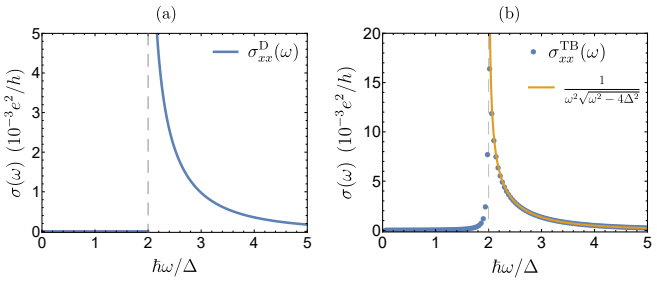


FIG. 3. Real part of the 2D optical conductivity in a superconductor carrying supercurrent. (a) Analytical expression for $\sigma_{aa}(\omega)$ for s-wave superconductor with a 2D Dirac fermion dispersion. As s-wave superconductors are fully gapped for small Cooper pair momentum, the optical conductivity only carries the interband contribution and remains gapped for $\hbar\omega < 2\Delta$. (b) Numerical results for $\sigma_{xx}(\omega)$ calculated using tight-binding model for a 2D layer. The solid line shows the $1/(\omega^2\sqrt{\omega^2-4\Delta^2})$ dependence that can be inferred from the analytical calculation without the vertex correction.

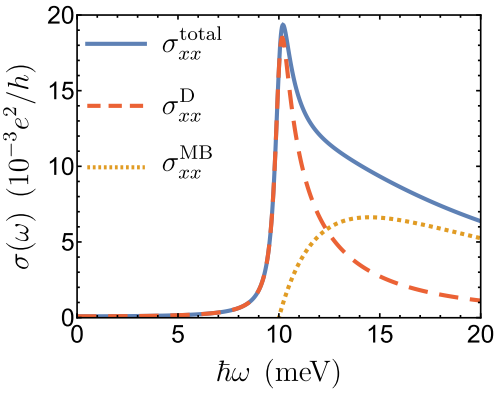


FIG. 4. Optical conductivity for superconducting Dirac surface state, with the parameters chosen to describe the surface state of $CaKFe_4As_4$ at $T = 1\,\mathrm{K}$, with $\Delta = 5\,\mathrm{mev}$, $v = 10^5\mathrm{m/s}$ and $\mu = 20\,\mathrm{meV}$ with $l/\xi_0 = 8$, for supercurrent that closes half of the superconducting gap. The yellow dotted line shows the corresponding theoretical Mattis-Bardeen contribution of the proximitized 2D Dirac surface state from impurity scattering, red dashed line shows the supercurrent-induced part, and blue solid line shows both contributions combined.

gaining better insight into the phenomenon. In this case we obtain the result including the vertex correction [24]:

$$\mathrm{Re}\,\sigma_{aa}^{D}(\omega) = \frac{e^2}{h}\frac{\pi}{4}\frac{\Delta}{\mu}\frac{\hbar^2 v^2 q_x^2 \Delta}{\hbar^2\omega^2\sqrt{\hbar^2\omega^2-4\Delta^2}}\Theta(\omega-2\Delta), \quad (10)$$

with $a = x, y$, which means the optical conductivity for the Dirac fermion case is equal in the directions parallel and perpendicular to the supercurrent. This expression, presented in Fig. 3(a), highlights several important characteristics of supercurrent-induced optical conductivity. First of all, since the supercurrent in this case only tilts the dispersion of quasiparticles, the energy separation of the two BdG branches of the spectrum at a given momentum $\mathbf{k}$ remains the same. Therefore, the minimal photon energy at which a transition can occur is still $2\Delta$ and optical conductivity remains zero for smaller energies. Moreover, the optical conductivity also has a $1/\sqrt{\hbar\omega-2\Delta}$ singularity at the gap boundary, which will correspond to a peak in experimentally relevant scenarios. The origin of this singularity is related to the density of states of a BCS superconductor, which contains precisely this type of singularity at the gap edges. Finally, $\mathrm{Re}\,\sigma_{aa}^{D}(\omega)$ depends quadratically on the Cooper pair momentum $\mathbf{q}$.

In the case of a tight-binding band described by Eq. (4) we cannot obtain an analytical result and have to rely on numerical calculation for the current-current correlation function with vertex correction as shown in Fig. 3(b). In numerical calculations we have used $t = 1$, $\mu = 0.9$, $\lambda = -1$, and $q_x = 0.025$. As mentioned above, approximating the band as parabolic would lead to no non-trivial optical response due to Galilean invariance. Nevertheless, calculation using bare current vertices can give additional insight into the functional form of frequency dependence, leaving the exact prefactor (dependent on the deviation from parabolic dispersion) to be determined numerically. As discussed in Supplemental Materials, the frequency dependence is $\sim 1/(\omega^2\sqrt{\omega^2-4\Delta^2})$ and can be precisely fitted to the numerical results as demonstrated in Fig. 3(b). This means that the results for tight-binding band share similarities with the Dirac fermion case, stemming from the same s-wave type of order parameter. Those features are the presence of the singularity at the gap edge and the absence of optical absorption inside of the gap. However, in contrast to the Dirac fermion case, here the optical conductivity in the direction perpendicular to the supercurrent ($\sigma_{yy}$) vanishes. This illustrates the impact of the normal state dispersion on the detailed characteristics of supercurrent-induced optical conductivity.

*Discussion.*— As presented above, the characteristics of supercurrent-induced optical conductivity vary considerably depending both on the nature of the underlying normal state as well as the type of the superconducting order parameter. As a consequence, optical conductivity with supercurrent present may serve as an important tool for characterizing the superconducting state. In particular, as the supercurrent flow can be introduced by applying external magnetic field and utilizing the Meissner effect, the anisotropies of both the normal state dispersion as well as the superconducting gap can be investigated using a vector magnet. As was shown in the $Bi_2Te_3/NbSe_2$ system [14], applying only 20 mT of in-plane field was sufficient to realize Doppler energy shift comparable to the superconducting gap. At the same time, that experiment has demonstrated that the screening supercurrent effects are sensitive to the magnetic field direction. Therefore, similar effects may be visible in the optical conductivity measurements. This could enable disentangling the var-

ious Fermi pockets that contribute to superconductivity in materials such as some iron-based superconductors, where superconductivity in bulk bands and Dirac surface states coincides. Moreover, since the characteristics of current-induced optical conductivity depend on the nature of the order parameter (e.g. d-wave superconductors due to the nodal order parameter will have a non-zero contribution inside the gap and a different singular behavior [24]), this method could also elucidate the nature of the superconducting state of various materials, including the recently studied moiré superconductors such as twisted bilayer and trilayer graphene [31, 32].

To estimate the visibility of the proposed effect, it is necessary to evaluate it in comparison to the Mattis-Bardeen optical conductivity $\sigma^{MB}$ that arises purely from impurity effects. As an example, we compare the theoretical estimates of the supercurrent-induced and impurity-driven optical conductivity for a clean Dirac surface state of an iron superconductor. We choose the parameters for the calculation based on the ARPES measurements of $CaKFe_4As_4$ [33]. While the superconducting behavior of iron superconductors is in general quite complex [34], the surface behavior should still be observable, even though it may be superimposed on top of the signal arising from the bulk superconductivity. Such surface results may for example be resolved due to the isotropic behavior of the conductivity components. The results of the comparison are presented in Fig. 4. The supercurrent-induced effect dominates over $\sigma^{MB}$ in the vicinity of the superconducting gap. This is the region where the difference between the two sources of interband transitions is the most apparent: while $\sigma^{MB}$ follows a Drude tail for large $\omega$, it gets suppressed at the gap edge. In contrast, supercurrent flow introduces singular behavior of $\sigma(\omega)$ at the gap edge, leading to the appearance of a sharp peak. Moreover, in real materials the optical conductivity will depend on the direction of the supercurrent with respect to the crystalline axes due to the corrections to the dispersion such as hexagonal warping [35]. Since both the magnitude of the peak as well as the anisotropy of optical conductivity can be controlled by the direction of the current (and in turn, the direction of the external magnetic field), it is possible to clearly distinguish current-enabled and impurity effects.

We can also compare the magnitude of the predicted effect to the present experiments on optical conductivity of superconductors. One such experiment investigated recently the supercurrent-induced Higgs mode activation [22]. In that experiment, the excess optical conductivity attributed to the supercurrent flow in NbN superconductor thin film was estimated to be on the order of 100 $(\Omega\,\mathrm{cm})^{-1}$ and is peaked for $\omega = 2\Delta$. In a 3D model, the current-induced optical conductivity is qualitatively similar to the 2D cases, but the value is rescaled by the Fermi wave vector $k_F$ to account for dimensionality [24]. As $k_F$ of NbN has been measured to be about 1.45 $\mathrm{Å}^{-1}$ [36], a 2D value of conductivity equal to 0.02 $e^2/h$ corresponds to about 110 $(\Omega\,\mathrm{cm})^{-1}$, right in line with the experimentally measured value. This means that the magnitude of the proposed effect is well within the experimental reach, and may have very well already been observed. However, convincingly separating our quasiparticle-based mechanism from one based on the Higgs mode in that experiment requires more detailed studies. Nevertheless, this demonstrates the experimental viability of the phenomenon we predict, enabling its application for investigation of the superconducting state.

In summary, we have shown that introducing supercurrent flow in a superconductor, either through applying external magnetic field or by direct transport current, can significantly affect its optical properties at photon energies close to the superconducting gap magnitude. The effect is generic, appearing independently of the nature of the normal states as well as of the pairing symmetry, yet it is sensitive to both of these important material characteristics. As such, supercurrent-driven optical conductivity may become a valuable tool in investigations of novel superconductors.

*Note added:* We thank Liang Fu and Philip Crowley for bringing our attention to the issue of Galilean invariance and its impact on the optical response. They have recently studied the optical response of s-wave superconductors with supercurrent using a different formalism than ours, and our results are in agreement in that case [37].

The authors also acknowledge helpful discussions with J. Orenstein. This work was supported by the Quantum Science Center (QSC), a National Quantum Information Science Research Center of the U.S. Department of Energy (DOE). M.P. received additional fellowship support from the Emergent Phenomena in Quantum Systems program of the Gordon and Betty Moore Foundation and J.E.M. acknowledges a Simons Investigatorship.

[1] J. Orenstein, Ultrafast spectroscopy of quantum materials, Physics Today **65**, 44 (2012).

[2] C. Giannetti, M. Capone, D. Fausti, M. Fabrizio, F. Parmigiani, and D. Mihailovic, Ultrafast optical spectroscopy of strongly correlated materials and high-temperature superconductors: A non-equilibrium approach, Advances in Physics **65**, 58 (2016).

[3] D. N. Basov, R. D. Averitt, D. van der Marel, M. Dressel, and K. Haule, Electrodynamics of correlated electron materials, Rev. Mod. Phys. **83**, 471 (2011).

[4] L. Degiorgi, G. Briceno, M. S. Fuhrer, A. Zettl, and P. Wachter, Optical measurements of the superconducting gap in single-crystal $K_3C_{60}$ and $Rb_3C_{60}$, Nature **369**, 541 (1994).

[5] A. V. Pronin, M. Dressel, A. Pimenov, A. Loidl, I. V. Roshchin, and L. H. Greene, Direct observation of the superconducting energy gap developing in the conductivity

spectra of niobium, Phys. Rev. B **57**, 14416 (1998).
[6] B. Gorshunov, C. Kuntscher, P. Haas, M. Dressel, F. Mena, A. Kuz'menko, D. van der Marel, T. Muranaka, and J. Akimitsu, Optical measurements of the superconducting gap in $MgB_2$, Eur. Phys. J. B **21**, 159 (2001).
[7] D. C. Mattis and J. Bardeen, Theory of the Anomalous Skin Effect in Normal and Superconducting Metals, Phys. Rev. **111**, 412 (1958).
[8] L. Leplae, Derivation of an expression for the conductivity of superconductors in terms of the normal-state conductivity, Phys. Rev. B **27**, 1911 (1983).
[9] W. Zimmermann, E. H. Brandt, M. Bauer, E. Seider, and L. Genzel, Optical conductivity of BCS superconductors with arbitrary purity, Physica C: Superconductivity **183**, 99 (1991).
[10] J. Ahn and N. Nagaosa, Theory of optical responses in clean multi-band superconductors, Nat Commun **12**, 1617 (2021).
[11] T. Xu, T. Morimoto, and J. E. Moore, Nonlinear optical effects in inversion-symmetry-breaking superconductors, Phys. Rev. B **100**, 220501 (2019).
[12] K. Takasan, T. Morimoto, J. Orenstein, and J. E. Moore, Current-induced second harmonic generation in inversion-symmetric Dirac and Weyl semimetals, Phys. Rev. B **104**, L161202 (2021).
[13] P. Fulde, Gapless Superconducting Tunneling-Theory, in *Tunneling Phenomena in Solids: Lectures Presented at the 1967/NATO Advanced Study Institute at Risö, Denmark*, edited by E. Burstein and S. Lundqvist (Springer US, Boston, MA, 1969) pp. 427–442.
[14] Z. Zhu, M. Papaj, X.-A. Nie, H.-K. Xu, Y.-S. Gu, X. Yang, D. Guan, S. Wang, Y. Li, C. Liu, J. Luo, Z.-A. Xu, H. Zheng, L. Fu, and J.-F. Jia, Discovery of segmented Fermi surface induced by Cooper pair momentum, Science 10.1126/science.abf1077 (2021).
[15] M. Papaj and L. Fu, Creating Majorana modes from segmented Fermi surface, Nat Commun **12**, 577 (2021).
[16] K. Takasan, S. Sumita, and Y. Yanase, Supercurrent-induced topological phase transitions, arXiv:2110.06959 [cond-mat] (2021), arXiv:2110.06959 [cond-mat].
[17] G. Volovik, Superconductivity with Lines of Gap Nodes - Density-of-States in the Vortex, Jetp Lett. **58**, 469 (1993).
[18] R. Mallozzi, J. Orenstein, J. N. Eckstein, and I. Bozovic, High-frequency electrodynamics of $Bi_2Sr_2CaCu_2O_{8+\delta}$: Nonlinear response in the vortex state, Phys. Rev. Lett. **81**, 1485 (1998).
[19] W. Kim, F. Marsiglio, and J. P. Carbotte, Microwave conductivity of a high-purity *d*-wave superconductor, Phys. Rev. B **70**, 060505 (2004).
[20] Z. Tagay, F. Mahmood, A. Legros, T. Sarkar, R. L. Greene, and N. P. Armitage, BCS *d*-wave behavior in the terahertz electrodynamic response of electron-doped cuprate superconductors, Phys. Rev. B **104**, 064501 (2021).
[21] A. Moor, A. F. Volkov, and K. B. Efetov, Amplitude Higgs Mode and Admittance in Superconductors with a Moving Condensate, Phys. Rev. Lett. **118**, 047001 (2017).
[22] S. Nakamura, Y. Iida, Y. Murotani, R. Matsunaga, H. Terai, and R. Shimano, Infrared Activation of the Higgs Mode by Supercurrent Injection in Superconducting NbN, Phys. Rev. Lett. **122**, 257001 (2019).
[23] A. Anthore, H. Pothier, and D. Esteve, Density of States in a Superconductor Carrying a Supercurrent, Phys. Rev. Lett. **90**, 127001 (2003).
[24] Additional details of the analytical calculation are available in Supplementary Materials.
[25] J. Bardeen, Critical Fields and Currents in Superconductors, Rev. Mod. Phys. **34**, 667 (1962).
[26] T. Yanagisawa and H. Shibata, Chapter 1 Optical Properties of Unconventional Superconductors, in *New Topics in Josephson Junction And Superconductivity Research*, edited by C. S. Winslow (Nova Science Pub Inc, New York, 2007).
[27] F. Horváth, M. Sigrist, and R. Hlubina, Current-carrying state of a nodal correlated superconductor, Phys. Rev. B **85**, 184527 (2012).
[28] P. Coleman, *Introduction to Many-Body Physics* (Cambridge University Press, Cambridge, 2015).
[29] Z. Dai and P. A. Lee, Optical conductivity from pair density waves, Phys. Rev. B **95**, 014506 (2017).
[30] Y. Nambu, Quasi-Particles and Gauge Invariance in the Theory of Superconductivity, Phys. Rev. **117**, 648 (1960).
[31] Y. Cao, V. Fatemi, S. Fang, K. Watanabe, T. Taniguchi, E. Kaxiras, and P. Jarillo-Herrero, Unconventional superconductivity in magic-angle graphene superlattices, Nature **556**, 43 (2018).
[32] Y. Cao, J. M. Park, K. Watanabe, T. Taniguchi, and P. Jarillo-Herrero, Pauli-limit violation and re-entrant superconductivity in moiré graphene, Nature **595**, 526 (2021).
[33] W. Liu, L. Cao, S. Zhu, L. Kong, G. Wang, M. Papaj, P. Zhang, Y.-B. Liu, H. Chen, G. Li, F. Yang, T. Kondo, S. Du, G.-H. Cao, S. Shin, L. Fu, Z. Yin, H.-J. Gao, and H. Ding, A new Majorana platform in an Fe-As bilayer superconductor, Nat Commun **11**, 5688 (2020).
[34] L.-H. Hu, P. D. Johnson, and C. Wu, Pairing symmetry and topological surface state in iron-chalcogenide superconductors, Phys. Rev. Research **2**, 022021 (2020).
[35] L. Fu, Hexagonal Warping Effects in the Surface States of the Topological Insulator Bi2Te3, Phys. Rev. Lett. **103**, 266801 (2009).
[36] S. P. Chockalingam, M. Chand, J. Jesudasan, V. Tripathi, and P. Raychaudhuri, Superconducting properties and Hall effect of epitaxial NbN thin films, Phys. Rev. B **77**, 214503 (2008).
[37] P. J. D. Crowley and L. Fu, Supercurrent induced resonant optical response, arXiv:2203.06192 [cond-mat] (2022), arXiv:2203.06192 [cond-mat].